A Numerical Solution to Full-Vector Electromagnetic Scattering by Three-Dimensional Nonlinear Bounded Dielectrics

Salvatore Caorsi, Andrea Massa, and Matteo Pastorino, *Member, IEEE*

Abstract—**This paper deals with electromagnetic scattering by nonlinear dielectric objects. In particular, a numerical approach is developed that is aimed at determining the distributions of the electromagnetic field vector inside a three-dimensional nonlinear, inhomogeneous, isotropic scatterer illuminated by a time-periodic incident electric field vector. An integral-equation formulation for the full-vector scattering problem is considered, and the nonlinear effect is taken into account by introducing equivalent sources and a Fourier-series representation. A system of integral equations (for each harmonic vector components and for the static term) is obtained that includes the internal electric field distribution as the unknown. After discretization, the solution is reduced to solving an algebraic system of nonlinear equations. Some preliminary numerical results are reported concerning scatterers that exhibit a specific (quadratic) dependence of the dielectric permittivity on the total electric field. The harmonic components of the scattered electric field outside the objects are also computed.**

I. Introduction

THE PROPAGATION of electromagnetic waves through solids is essentially a quantum-mechanical phenomenon, as it involves interactions between energy quanta and matter. However, the description of such propagation in terms of classical field theory is always useful in the context of macroscopic interactions. Unfortunately, in the presence of nonlinear media, it is in general very difficult to predict nonlinear electromagnetic phenomena by general solutions of the Maxwell equations. For this reason, in the past particular solutions were proposed in order to explain such phenomena. In this context, the study of electromagnetic wave propagation [1] was aimed, for example, at defining the conditions under which shock waves may form and propagate [2] and at analyzing the behaviors of solitary waves and soliton waves, which are solitary waves that develop and interact without losing their identity [3]. Many types of solitons in various physical media were described (e.g., in water as well as optical waveguide) [4]–[7].

Nonlinear wave propagation and scattering were the subjects of fundamental books in the fields of nonlinear optics [8] [9] and nonlinear electromagnetics [10]. These books gave an idea of the broad spectrum of possible applications (see also [11]). To study the electromagnetic field in the presence of nonlinear media, approximate solutions were very often adopted, using both numerical and analytical techniques. For example, in [12] the perturbation technique was applied to electromagnetic waves in waveguides and cavities filled with nonlinear media. The authors assumed isotropic media where the dielectric permittivity and the magnetic permeability were dependent on the amplitudes of the electric and magnetic fields, respectively. Others used a functional approach based on the Volterra series [13] (which is the functional analogous to the Taylor series), for example, to characterize whistler-mode propagation in plasma [14] and to study nonlinearly loaded antennas [15].

However, in most cases, propagation along infinite or semi-infinite nonlinear media was considered, while more work needs to be done on the interactions between electromagnetic waves and nonlinear dielectrics of limited dimensions (i.e., electromagnetic scattering problems).

This topic was addressed by D. Censor from a systematic point of view [16], [17]. He considered weak nonlinearities described by Volterra series, and analyzed the scattering from cylinders and spheres. In [18], [19], the authors presented a solution to the electromagnetic scattering of obliquely incident plane waves from homogeneous, nonlinear, anisotropic cylinders. They used plane waves of unit amplitude as incident fields and circular cylinders whose radii were fractions of the wavelength related to the fundamental frequency.

This paper presents a numerical approach to the computation of the electromagnetic field vector scattered by three-dimensional, bounded, inhomogeneous, isotropic, dielectric objects with nonlinear characteristics (direct scattering problem). The dielectric permittivity depends on the electric field inside an object and hence on the interaction mechanism between the incident electromagnetic field and the nonlinear material.

In particular, the purpose is to explore a numerical technique to determine the electromagnetic field distributions inside and outside a nonlinear body of arbitrary shape. To this end, we develop an integral-equation formalism in which nonlinear effects are taken into account and analytically represented in terms of equivalent sources. The moment method [20] is used to discretize the resulting set of coupled integral equations. The problem solution is finally reduced to the solution of a system of nonlinear algebraic equations.

Manuscript received May 19, 1993; revised April 1, 1994.

The authors are with the Department of Biophysical and Electronic Engineering, University of Genoa, 16145 Genova, Italy.

IEEE Log Number 9407302.

The mathematical formulation of the approach is presented in Section II, and the results of some numerical simulations are reported in Section III.

II. Mathematical Formulation

Let us consider a bounded region D, which is occupied by a nonlinear bounded dielectric object characterized by a dielectric permittivity $\varepsilon_{\mathrm{NL}}(\mathbf{r},t)$($\mathbf{r}$: position vector; t: time variable), which depends on the electric field inside the object through the relationship:

$$\varepsilon_{\mathrm{NL}}(\mathbf{r},t)=\varepsilon_0[\varepsilon_b(\mathbf{r})+\mathcal{L}\{\mathbf{E}(\mathbf{r},t)\}] \tag{1}$$

where $\mathbf{E}(\mathbf{r},t)$ is the total electric field vector, $\varepsilon_b(\mathbf{r})$ is the linear component of the relative dielectric permittivity and $\mathcal{L}\{\mathbf{E}(\mathbf{r},t)\}$ denotes an operator that is assumed to fulfill the constraint of not modifying the scalar nature of the dielectric permittivity (i.e., the isotropic nature of the dielectric object) and to be a periodic function expansible in Fourier series. Further, the dielectric object has a magnetic permeability equal to μ_0 (we neglect the possibility that the nonlinearity of the dielectric permittivity may influence the magnetic permeability). The region outside D is a homogeneous, isotropic, nondissipative, boundless space region. The dielectric characteristics of this region are represented by the dielectric permittivity ε_0 and the magnetic permeability μ_0. Moreover, $\mathbf{E}^i(\mathbf{r},t)$ and $\mathbf{H}^i(\mathbf{r},t)$ stand for the incident electromagnetic field vectors produced by an electromagnetic source in the absence of scattering objects, i.e., in the presence of an entirely homogeneous region characterized by the dielectric constants μ_0 and ε_0.

At each point, the total electromagnetic field vectors, $\mathbf{E}(\mathbf{r},t)$ and $\mathbf{H}(\mathbf{r},t)$, satisfy the Maxwell equations:

$$\nabla\times\mathbf{E}(\mathbf{r},t)=-\mu_0\frac{\partial}{\partial t}\{\mathbf{H}(\mathbf{r},t)\} \tag{2}$$

$$\nabla\times\mathbf{H}(\mathbf{r},t)=\frac{\partial}{\partial t}\{\varepsilon(\mathbf{r},t)\mathbf{E}(\mathbf{r},t)\} \tag{3}$$

and Sommerfeld's radiation conditions.

The presence of the object can be taken into account by solving a suitable equivalent problem in which the scattering object is replaced by an equivalent current density distribution that extends to a domain that coincides with the region D, but that is characterized by the same dielectric parameters as the propagation medium. By definition, this equivalent current density must be such as to produce, inside the region D, an electromagnetic field equal to the one resulting from the scattering by the medium inhomogeneity represented by the nonlinear object. It follows that the electromagnetic field now fulfils the following [21]:

$$\nabla\times\mathbf{E}(\mathbf{r},t)=-\mu_0\frac{\partial}{\partial t}\{\mathbf{H}(\mathbf{r},t)\} \tag{4}$$

$$\nabla\times\mathbf{H}(\mathbf{r},t)=\varepsilon_0\frac{\partial}{\partial t}\{\mathbf{E}(\mathbf{r},t)\}+\mathbf{J}_{\mathrm{eq}}(\mathbf{r},t) \tag{5}$$

where

$$\begin{aligned}\mathbf{J}_{\mathrm{eq}}(\mathbf{r},t)&=\varepsilon_0\frac{\partial}{\partial t}\{[\varepsilon_b(\mathbf{r})-1]\mathbf{E}(\mathbf{r},t)\}+\varepsilon_0\frac{\partial}{\partial t}\{\mathcal{L}\{\mathbf{E}(\mathbf{r},t)\}\mathbf{E}(\mathbf{r},t)\}\\&=\mathbf{J}_L(\mathbf{r},t)+\mathbf{J}_{\mathrm{NL}}(\mathbf{r},t)\end{aligned} \tag{6}$$

If the electromagnetic coupling between the electromagnetic source and the scattering object is negligible, the total electric and magnetic field vectors at each point can be expressed as:

$$\mathbf{E}(\mathbf{r},\mathbf{t})=\mathbf{E}^{\mathbf{i}}(\mathbf{r},\mathbf{t})+\mathbf{E}^{\mathbf{s}}(\mathbf{r},\mathbf{t}) \tag{7}$$

$$\mathbf{H}(\mathbf{r},\mathbf{t})=\mathbf{H}^{\mathbf{i}}(\mathbf{r},\mathbf{t})+\mathbf{H}^{\mathbf{s}}(\mathbf{r},\mathbf{t}) \tag{8}$$

where $\mathbf{E}^s(\mathbf{r},t)$ and $\mathbf{H}^s(\mathbf{r},t)$ denote the electric and magnetic field vectors scattered by the dielectric object, and satisfy the equations:

$$\nabla\times\mathbf{E}^s(\mathbf{r},t)=-\mu_0\frac{\partial}{\partial t}\{\mathbf{H}^s(\mathbf{r},t)\} \tag{9}$$

$$\nabla\times\mathbf{H}^s(\mathbf{r},t)=\varepsilon_0\frac{\partial}{\partial t}\{\mathbf{E}^s(\mathbf{r},t)\}+\mathbf{J}_{\mathrm{eq}}(\mathbf{r},t) \tag{10}$$

where $\mathbf{J}_{\mathrm{eq}}(\mathbf{r},t)$ is still given by (6). As is well known, from (9) and (10) it is possible to derive the inhomogeneous wave equation:

$$\nabla\times\nabla\times\mathbf{E}^s(\mathbf{r},t)+\mu_0\varepsilon_0\frac{\partial}{\partial t}\{\mathbf{E}^s(\mathbf{r},t)\}=-\mu_0\frac{\partial}{\partial t}\{\mathbf{J}_{\mathrm{eq}}(\mathbf{r},t)\} \tag{11}$$

Then, under the hypotheses made on the incident electric field vector and on the nonlinear permittivity, we can expand $\mathbf{E}(\mathbf{r},t)$, $\mathbf{E}^s(\mathbf{r},t)$ and $\mathcal{L}\{\mathbf{E}(\mathbf{r},t)\}$ in Fourier series with the fundamental pulsation $\omega_0=2\pi f_0$ (f_0 being the fundamental frequency of the incident field), as follows

$$\mathbf{E}(\mathbf{r},t)=\sum_{a=-\infty}^{+\infty}\mathbf{E}_a(\mathbf{r})\exp(j\omega_a t),\qquad \omega_a=a\omega_0\ \text{(a integer)} \tag{12}$$

$$\mathbf{E}^s(\mathbf{r},t)=\sum_{a=-\infty}^{+\infty}\mathbf{E}_a^s(\mathbf{r})\exp(j\omega_a t) \tag{13}$$

$$\mathcal{L}\{\mathbf{E}(\mathbf{r},\mathbf{t})\}=\sum_{a=-\infty}^{+\infty}O_a(\mathbf{r})\exp(j\omega_a t) \tag{14}$$

where $O_a(\mathbf{r})$ denotes the a-th (scalar) term of the Fourier expansion of $\mathcal{L}\{\mathbf{E}(\mathbf{r},t)\}$ that can be made explicit once the nonlinear operator has been specified. From (12) and (14), we obtain the following relation:

$$\mathcal{L}\{\mathbf{E}(\mathbf{r},t)\}\mathbf{E}(\mathbf{r},t)=\sum_{a=-\infty}^{+\infty}\mathbf{T}_a(\mathbf{r})\exp(j\omega_a t) \tag{15}$$

where

$$\mathbf{T}_a(\mathbf{r})=\sum_{a_1=-\infty}^{+\infty}\sum_{a_2=-\infty}^{+\infty}\gamma_{a_1,a_2}^{a}O_{a_1}(\mathbf{r})\mathbf{E}_{a_2}(\mathbf{r})\quad(a_1,a_2\ \text{integer}) \tag{16}$$

and $\gamma_{a_1,a_2}^{a}=1$ if $a_1+a_2=a$, $\gamma_{a_1,a_2}^{a}=0$ otherwise.

It should be noted that, in this relation, each vector $\mathbf{T}_a(\mathbf{r})$ generally depends on all the harmonic components of the electric field. From (6), it follows that the vector $\mathbf{T}_a(\mathbf{r})$ is proportional (by a factor $1/j\omega_a\varepsilon_0$) to the a-th Fourier components of the nonlinear part of the equivalent current

density. At this point, it is possible to substitute (9), (13) and (15) into (11), thus obtaining:

$$\sum_{a=-\infty}^{+\infty} \exp(j\omega_a t)\{\nabla \times \nabla \times \mathbf{E}_a^s(\mathbf{r}) - \omega_a^2 \mu_0 \varepsilon_0 \mathbf{E}_a^s(\mathbf{r})\} = \sum_{a=-\infty}^{+\infty} \exp(j\omega_a t) \times \{\omega_a^2 \mu_0 \varepsilon_0 [\varepsilon_b(\mathbf{r}) - 1]\mathbf{E}_a(\mathbf{r}) + \omega_a^2 \mu_0 \varepsilon_0 \mathbf{T}_a(\mathbf{r})\} \tag{17}$$

From (17), one can deduce that each harmonic component satisfies he inhomogeneous wave equation:

$$\nabla \times \nabla \times \mathbf{E}_a^s(\mathbf{r}) - k_a^2 \mathbf{E}_a^s(\mathbf{r}) = k_a^2 [\varepsilon_b(\mathbf{r}) - 1]\mathbf{E}_a(\mathbf{r}) + k_a^2 \mathbf{T}_a(\mathbf{r}) \tag{18}$$

where $k_a = \omega_a \sqrt{\mu_0 \varepsilon_0}$ (i.e., wavenumber for the pulsation w_a).

From this relation, it appears evident that the presence of the term $\mathbf{T}_a(\mathbf{r})$ on the right-hand side indicates the dependence of the generic harmonic term for the electromagnetic scattering on the mutual coupling among the different vectors related to the various frequencies. In particular, for $\mathcal{L}\{\mathbf{E}(\mathbf{r}, t)\} = 0$, that is, in the case of linear conditions, all terms $\mathbf{T}_a(\mathbf{r})$ are zero, and (18) is equivalent to the well-known equation for direct scattering in linear problems [20].

Therefore, a formal solution to (18), that is, the expression for the a-th generic component ($a \neq 0$) of the scattered electric field vector, can be written as:

$$\mathbf{E}_a^s(\mathbf{r}) = -\int_D k_a^2 [\varepsilon_b(\mathbf{r}') - 1]\mathbf{E}_a(\mathbf{r}') \cdot G_0(\mathbf{r}/\mathbf{r}', k_a) d\mathbf{r}' - \int_D k_a^2 \mathbf{T}_a(\mathbf{r}') \cdot G_0(\mathbf{r}/\mathbf{r}', k_a) d\mathbf{r}' \tag{19}$$

where $G_0(\mathbf{r}/\mathbf{r}', k_a)$ denotes the dyadic Green function for free space [22]:

$$G_0(\mathbf{r}/\mathbf{r}', k_a) = \frac{1}{4\pi}\left[\mathbf{I} + \frac{1}{k_a^2}\nabla\nabla\right]\frac{\exp(-jk_a|\mathbf{r} - \mathbf{r}'|)}{|\mathbf{r} - \mathbf{r}'|} \tag{20}$$

where $\mathbf{I}$ is the unit dyadic.

For the 0-th harmonic term, for which $k_a = 0$ (static component), it is possible to consider the following expression for the polarization vector:

$$\mathbf{P}_0(\mathbf{r}) = \varepsilon_0 [\varepsilon_b(\mathbf{r}) - 1]\mathbf{E}_0(\mathbf{r}) + \varepsilon_0 \mathbf{T}_0(\mathbf{r}) \tag{21}$$

from which the following relation for the 0-th component of the scattered electric field can be derived:

$$\mathbf{E}_0^s(\mathbf{r}) = \frac{1}{4\pi\varepsilon_0}\oint_S \frac{\mathbf{r} - \mathbf{r}'}{|\mathbf{r} - \mathbf{r}'|^3} \times \{\varepsilon_0[\varepsilon_b(\mathbf{r}') - 1]\mathbf{E}_0(\mathbf{r}') - \varepsilon_0 \mathbf{T}_0(\mathbf{r}')\} \cdot \hat{\mathbf{n}} d\mathbf{r}' - \frac{1}{4\pi\varepsilon_0}\int_D \frac{\mathbf{r} - \mathbf{r}'}{|\mathbf{r} - \mathbf{r}'|^3}\nabla \times \{\varepsilon_0[\varepsilon_b(\mathbf{r}') - 1]\mathbf{E}_0(\mathbf{r}') - \varepsilon_0 \mathbf{T}_0(\mathbf{r}')\} d\mathbf{r}' \tag{22}$$

where S is the surface including the domain D, and $\hat{\mathbf{n}}$ is the outward normal unit vector.

Equations (19) and (22) indicate an explicit functional relationship among the harmonic components of the scattered electric field vector. If we consider a finite number, A, of harmonic components, (19) can be rewritten for each value of a ($a \neq 0$), thus leading to a system of $A + 1$ vector integral-differential equations (for $a = 0$, consider (22)). This system can be discretized by the moment method [20]. To this end, we expand all components E_{a,x_p} and T_{a,x_p}, $p = 0, 1, 2$ (we assume $(x_0, x_1, x_2) = (x, y, z)$), into sums of N basis functions with the coefficients E_{a,x_p}^n and T_{a,x_p}^n ($n = 1, \ldots, N$), and we consider N suitable testing functions $w_m, m = 1, \ldots, N$. In this paper, we utilize, for simplicity, rectangular pulse functions as basis functions and Dirac deltas as testing functions. Under such assumptions, from (22) we obtain

$$E_{0,x_p}^m = \frac{1}{4\pi}\sum_{n=1}^{N}\sum_{q=0}^{2}\left\{(\varepsilon_b(\mathbf{r}_n) - 1)E_{0,x_q}^n + T_{0,x_q}^n\right\} \times \left\{\frac{x_{p,m} - x_{p,n} - \frac{d_{n_q}}{2}\delta_{pq}}{|\mathbf{r}_m - \mathbf{r}_n - \frac{d_{n_q}}{2}\hat{\mathbf{q}}|^3} - \frac{x_{p,m} - x_{p,n} - \frac{d_{n_q}}{2}\delta_{pq}}{|\mathbf{r}_m - \mathbf{r}_n - \frac{d_{n_q}}{2}\hat{\mathbf{q}}|^3}\right\}\Delta S_{n_q} \quad p = 0, \ldots, 2 \quad m = 1, \ldots, N \tag{23}$$

where $\mathbf{r}_n = (x_{0,n}, x_{1,n}, x_{2,n})$ denotes the position vector related to the center of the n-th subvolume of D, ΔS_{n_q} represents the area of the face of the n-th subdomain orthogonal to the q-axis, d_{n_q} is the edge of the same subdomain parallel to the q direction and, finally, δ_{pq} stands for the Kronecker symbol ($\delta_{pq} = 1$ if $p = q$, $\delta_{pq} = 0$ otherwise).

Application of the moment method to (19) yields:

$$\sum_{q=0}^{2}\sum_{n=1}^{N}\left\{G_{a,x_p,x_q}^{mn}\right\}E_{a,x_q}^n + \sum_{q=0}^{2}\sum_{n=1}^{N}\left\{\Lambda_{a,x_p,x_q}^{mn}\right\}T_{a,x_q}^n = -e_{a,x_p}^m \quad m = 1, \ldots, N \quad p = 0, \ldots, 2 \quad a = 1, \ldots, A \tag{24}$$

where e_{a,x_p}^m is the x_p Cartesian component of the a-th harmonic term of the known incident electric field, $\mathbf{E}^i(\mathbf{r})$, evaluated for $\mathbf{r} = \mathbf{r}_m$. In (24), $G_{a.x_p,x_q}^{mn}$ and G_{a,x_p,x_q}^{mn} are given by:

$$\begin{cases} G_{a,x_p,x_q}^{mn} = \tilde{G}_{a,x_p,x_q}^{mn} - \delta_{pq}\delta_{mn}\left[1 + \frac{\tau_a(\mathbf{r_n})}{3j\omega_a\varepsilon_0}\right] \\ \tilde{G}_{a,x_p,x_q}^{mn} = \tau_a(\mathbf{r}_n)\left[\mathrm{PV}\left\{\int_{V_a} G_{a,pq}(\mathbf{r}_m/\mathbf{r}', k_a)d\mathbf{r}'\right\}\right] \end{cases} \tag{25}$$

$$\begin{cases} \Lambda_{a,x_p,x_q}^{mn} = \hat{\Lambda}_{a,x_p,x_q}^{mn} - \frac{1}{3}\delta_{pq}\delta_{mn} \\ \hat{\Lambda}_{a,x_p,x_q}^{mn} = j\omega_a\varepsilon_0\left[\mathrm{PV}\left\{\int_{V_a} G_{a,pq}(\mathbf{r}_m/\mathbf{r}', k_a)d\mathbf{r}'\right\}\right] \end{cases} \tag{26}$$

where $\tau(\mathbf{r}_n) = j\omega_a\varepsilon_0[\varepsilon_b(\mathbf{r}_n) - 1]$ and PV indicates the principal value of the integral.

Equations (25) and (26) can be explicitly derived as in [23] for the linear case, taking into account the Van Bladel theory for the principal value [24]. As a result, we obtain (27), shown at the bottom of the page, and

$$\Lambda^{mn}_{a,x_p,x_q} = \begin{cases} \frac{-j\omega_a\mu_0 k_a(j\omega_a\varepsilon_0)\Delta V_n \exp(-j\gamma_{mn})}{4\pi(\gamma_{mn})^2} \\ \quad \times\left\{\left[(\gamma_{mn})^2 - 1 - j\gamma_{mn}\right]\delta_{pq} \right. \\ \quad \left. + \xi^{mn}_{x_p}\xi^{mn}_{x_q}\left[3 - (\gamma_{mn})^2 + 3j\gamma_{mn}\right]\right\} & m \neq n \\ \delta_{pq}\left\{-\frac{2j\omega_a\tau\mu_0}{3k_a^2}\right. \\ \quad \times\left[(1 + jk_a\rho_n)\exp(-jk_a\rho_n) - 1\right] \\ \quad \left. -\left[1 + \frac{\tau_a(\mathbf{r}_n)}{3j\omega_a\varepsilon_0}\right]\right\} & m = n \end{cases} \tag{28}$$

where $\gamma_{mn} = ak_0|\mathbf{r}_m - \mathbf{r}_n|, \xi^{mn}_{x_p} = \frac{x_{p,m} - x_{p,n}}{|\mathbf{r}_m - \mathbf{r}_n|}, \rho_n = \sqrt[3]{\frac{3\Delta V_n}{4\pi}}$ and ΔV_n is the volume of the n-th subdomain.

By using (23) and (24), we obtain a system of $(A+1)\times N\times 3$ scalar algebraic equations that can be solved by means of a suitable computation algorithm. This system allows one to determine an approximate distribution of the scalar harmonic components of the scattered electric field inside the scatterer. Starting from such an approximate distribution, the values of the harmonic components of the total electric field vector at each point outside the scatterer can be easily obtained by numerically calculating the integral on the right-hand side of the equation:

$$\mathbf{E}_a(\mathbf{r}) = \mathbf{E}^i_a(\mathbf{r}) + j\omega_a\mu_0 \int_D \left[\tau_a(\mathbf{r})\mathbf{E}_a(\mathbf{r}) + j\omega_a\varepsilon_0\mathbf{T}_a(\mathbf{r})\right] \times G_0(\mathbf{r}/\mathbf{r}', k_a)d\mathbf{r}' \qquad a = 1,\ldots,A \tag{29}$$

III. Numerical Examples

In this section, we present the results of some numerical simulations performed mainly in order to explore the possibility of determining the harmonic components of the electric field vectors inside nonlinear dielectric scatterers. As an example, we considered a dielectric scatterer, namely, a parallelepiped, whose volume was $\lambda_0/15\times\lambda_0/30\times\lambda_0/15$, λ_0 being the free-space wavelength related to the fundamental frequency. The object was assumed to be homogeneous in its linear part of the dielectric permittivity, lossless and nonmagnetic. Moreover, we assumed the nonlinear operator $\mathcal{L}\{\mathbf{E}(\mathbf{r},t)\}$ in relation (1) to be given by:

$$\mathcal{L}\{\mathbf{E}(\mathbf{r},t)\} = \alpha_2|\mathbf{E}(\mathbf{r},t)|^2 \tag{30}$$

where α_2 is a real coefficient, and $|\mathbf{E}(\mathbf{r},\mathbf{t})|$ stands for the amplitude of the electric field vector. Under such assumptions, the nonlinear dielectric permittivity turns out to be dependent on the electromagnetic power. According to (1), the expression for equivalent dielectric permittivity is:

$$\varepsilon_{\mathrm{NL}}(\mathbf{r},t) = \varepsilon_0\left\{\varepsilon_b + \alpha_2|\mathbf{E}(\mathbf{r},t)|^2\right\} \tag{31}$$

The object was illuminated by an incident electric field represented by two uniform plane waves of unit amplitude, at the frequencies f_0 and $2f_0$. The two waves propagated in the $\hat{z}$ direction, normal to one of the smallest sides of the scatterer, and the electric field vector was polarized in the $\hat{y}$ direction parallel to the smallest edge (to save space, the geometrical configuration is shown in the upper left portion of Fig. 6(a)). For this example, we used a frequency $f_0 = 1$ GHz, and the dimensions of the object were chosen such as to be comparable with the wavelengths of the fundamental and some harmonic components in order that the scattering phenomena might be significant. In addition, the object dimensions were fixed taking into account the need for a numerical discretization based on the criteria for an accurate usage of block models [20] (which require the field not to vary too much inside each cell), at least for the first harmonic vector components.

We considered the generation of six harmonic components at the frequencies $af_0, a = 0,\ldots,A, A = 6$ ($a = 0$ gives the static field), and we assumed $N = 4$. We obtained a system of $(A+1)\times N\times 3$ coupled scalar nonlinear algebraic equations, in which the unknown terms were the coefficients E^m_{a,x_p}. This system was solved by using the iterative Wolfe method [25].

As an example, Fig. 1(a) illustrates the amplitude behavior of the harmonic components of the copolarized scattered electric field vector (y-polarized), $|E^k_{a,y}|, a = 1,\ldots,A, A = 6$, versus various significant values of the nonlinear index α_2, in the range 0.0 to 0.1, for the k-th subdomain (with $\mathbf{r}_k = (\lambda_0/60, 0, -\lambda_0/60)$) and for a linear part of the relative dielectric permittivity $\varepsilon_b = 2.0$ (for this small value of ε_b, the nonlinear part of the dielectric permittivity becomes significant). The obtained values of the amplitude of the scattered electric field, for $\alpha_2 = 0.0$, coincide with those obtained by the authors (as a consistency check) by using the moment method [20] for direct scattering by linear dielectrics. Fig. 1(b) gives the amplitudes of the harmonic components of the copolarized scattered electric field vector (y-polarized), $|E^h_{a,y}|, a = 1,\ldots,A, A = 6$, for the h-th subdomain (with $\mathbf{r}_h = (\lambda_0/60, 0, -\lambda_0/60)$), versus various values of the linear part of the relative dielectric permittivity of the scatterer. In this case, we fixed $\alpha_2 = 0.1$. As expected, the amplitudes of

$$G^{mn}_{a,x_p,x_q} = \begin{cases} \frac{-j\omega_a\mu_0 k_a\tau_a(\mathbf{r}_n)\Delta V_n \exp(-j\gamma_{mn})}{4\pi(\gamma_{mn})^2}\left\{\left[(\gamma_{mn})^2 - 1 - j\gamma_{mn}\right]\delta_{pq} \right. \\ \quad \left. + \xi^{mn}_{x_p}\xi^{mn}_{x_q}\left[3 - (\gamma_{mn})^2 + 3j\gamma_{mn}\right]\right\} & m \neq n \\ \delta_{pq}\left\{-\frac{2j\omega_a\tau_a(\mathbf{r}_n)\mu_0}{3k_a^2}\left[(1 + jk_a\rho_n)\exp(-jk_a\rho_n) - 1\right]\right. \\ \quad \left. -\left[1 + \frac{\tau_a(\mathbf{r}_n)}{3j\omega_a\varepsilon_0}\right]\right\} & m = n \end{cases} \tag{27}$$

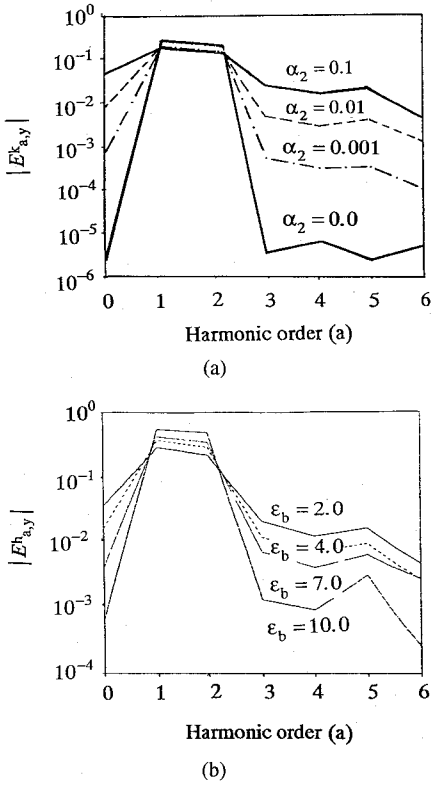

Fig. 1. Amplitudes of the harmonic components of the scattered electric field (coefficients $|E^m_{a,y}|$): (a) versus thenonlinear parameter α_2, for $\varepsilon_b = 2.0, m = k, \mathbf{r}_k = (\lambda_0/60, 0, -\lambda_0/60), A = 6$; (b) versus the linear part of the dielectric permittivity ε_b, for $\alpha_2 = 0.1, m = h, A = 6$.

the higher harmonic components decreased as the linear part of the dielectric permittivity increased, for the nonlinear effect was hidden by the linear part of the dielectric permittivity. Both Fig. 1(a) and (b) shows the generation of a rather significant static component, which the proposed approach is able to take into account. Once the coefficients $E^m_{a,x_p}, a = 0, \ldots, A, p = 0, \ldots, 2, m = 1, \ldots, N$, were obtained, the following quantity was computed:

$$\varepsilon^m_{\mathrm{eq}}(t) = \varepsilon_0 \left\{ \varepsilon_b(\mathbf{r}_m) + \alpha_2 \left| \sum_{a=-A}^{A} \sum_{p=0}^{2} E^m_{a,x_p} \exp(j\omega_a t)\hat{\mathbf{x}}_p + \sum_{a=-A}^{A} \sum_{p=0}^{2} e^m_{a,x_p} \exp(j\omega_a t)\hat{\mathbf{x}}_p \right|^2 \right\} \quad (32)$$

which can be viewed as an "equivalent" relative dielectric permittivity, of course, time-dependent. $\varepsilon^m_{\mathrm{eq}}(t)$ gives the approximate values of $\varepsilon_{\mathrm{NL}}(\mathbf{r}, t)$ in relation (1), for $\mathbf{r} = \mathbf{r}_m$.

Fig. 2(a) shows (for the specific incident electric field used) the behavior of $\varepsilon^k_{\mathrm{eq}}$ over a time interval corresponding to t_0 (i.e., the period of the fundamental component f_0), for a subdomain with $\mathbf{r}_k = (\lambda_0/60, 0, -\lambda_0/60)$, and for different values of the index α_2. Fig. 2(b) gives the plot of $\varepsilon^h_{\mathrm{eq}}$ (for the same time interval) versus various values of the linear part of the dielectric permittivity, for $\alpha_2 = 0.1$. One can observe that, as ε_b increases, the nonlinear effect tends to disappear, and $\varepsilon^h_{\mathrm{eq}}$ tends to assume constant values.

On the basis of the approximate internal electric field distribution, the external field was computed through relation

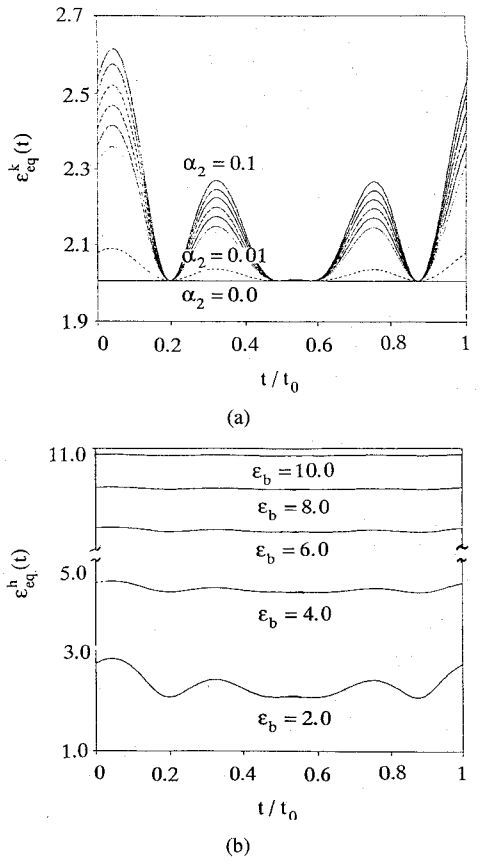

Fig. 2. Behavior of the equivalent dielectric permittivity $\varepsilon^m_{\mathrm{eq}}(t)$ as a function of time (relation (30)): (a) for various values of $\alpha_2(\varepsilon_b = 2.0, m = k, \mathbf{r}_k = (\lambda_0/60, 0, -\lambda_0/60), A = 6)$; (b) for various values of ε_b ($\alpha_2 = 0.1, m = h, \mathbf{r}_k = (\lambda_0/60, 0, -\lambda_0/20), A = 6$). t_0 is the period of the fundamental component at the frequency f_0.

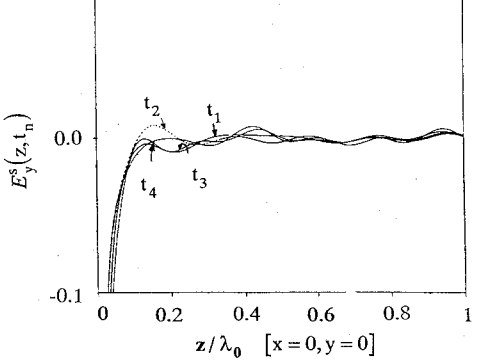

Fig. 3. Scattered electric field (y-component) along the propagation axis ($x = 0, y = 0$), for $\alpha_2 = 0.1, \varepsilon_b = 2.0, A = 6, t_n = (n-1)t_0/4$.

(29). The following figures give the field values at points along the propagation axis. One-thousand points were considered. Fig. 3 shows the behaviors of the time-dependent copolarized components of the scattered electric field vector, for $x = 0, y = 0$ and $0 < z \leq \lambda_0$, and for $t = t_n$, where $t_n = (n-1)t_0/4$. In this case, we assumed $\varepsilon_b = 2.0$ and $\alpha_2 = 0.1$. Fig. 4(a) shows the behaviours of the same components of the scattered electric field for two different values of the nonlinear parameter α_2, that is, $\alpha_2 = 0.01$ and 0.1, for $t = t_2$; Fig. 4(b) gives the same values for $t = t_4$. As

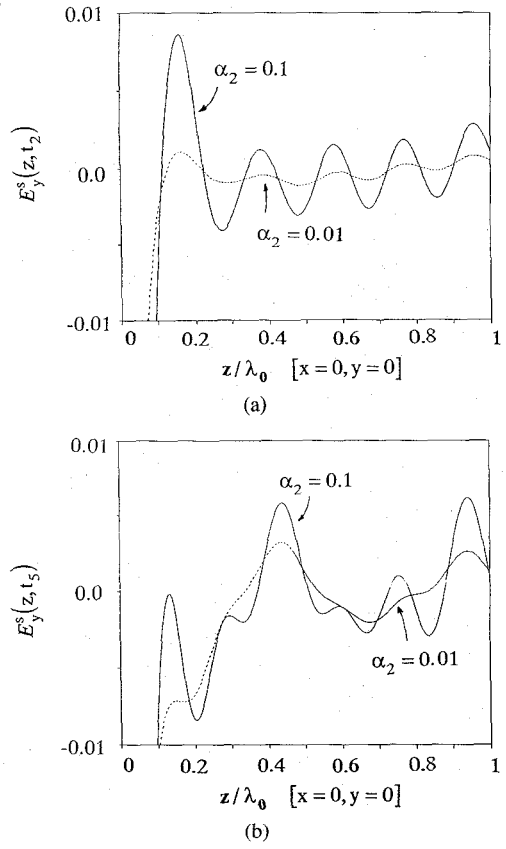

Fig. 4. Scattered electric field (y-component) along the propagation axis ($x = 0, y = 0$), for $\alpha_2 = 0.1$ and $0.01, \varepsilon_b = 2.0, A = 6$. (a) $t = t_2$; (b) $t = t_4$.

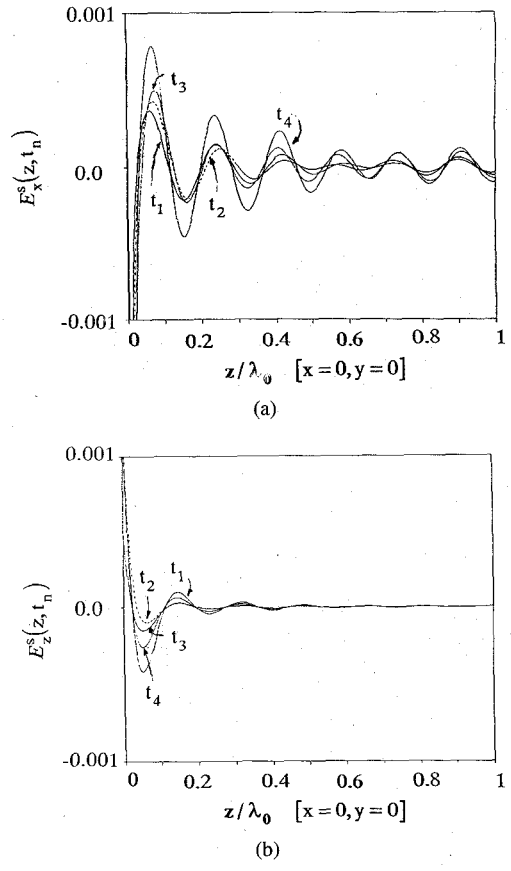

Fig. 5. Copolarized scattered electric field components along the propagation axis ($x = 0, y = 0$): (a) x-component; (b) z-component. We assumed $\alpha_2 = 0.1, \varepsilon_b = 2.0, A = 6, t_n = (n-1)t_0/4$.

an example, Fig. 5 gives the cross-polarized (x-polarized and z-polarized) components of the scattered electric field vector, for various values of t_n and for $\alpha_2 = 0.1$. As can be seen, due to the simple geometrical configuration considered and to the assumed isotropy of the medium, the amplitudes of these components are very small. Finally, a pictorial representation of the amplitude of the electric field forward-scattered on the $[xz]$ plane, $y = 0$, is presented. To cover a square area, 256 points were used, equally spaced ($\lambda_0/100$). Only the quadrant $x \geq 0$ was used, for symmetry reasons. Fig. 6(a) shows the amplitude of the static component $E_0(\mathbf{r}_s), \mathbf{r}_s = (x_s, 0, z_s)$; the fundamental component is plotted in Fig. 6(b), the second harmonic in Fig. 6(c), the third harmonic in Fig. 6(d), and the fourth harmonic in Fig. 6(e). The two computed higher-order components are not given. Each figure gives values for $\varepsilon_b = 2.0$ and for $\alpha_2 = 0.01$ and 0.1. In the numerical computations for the above simulations, Wolfe's algorithm was started by assuming that an initial solution for the harmonic components of the scattered electric field vectors was given by sequences (for the real and imaginary parts) of independent stochastic variables characterized by uniform distributions between -1 and $+1$ (V/m). This was an arbitrary choice, justified by the incident-field strength. Of course, if the linear scattering solution had been used as an initial solution, a fast convergence might have been reached. Whenever the obtained solution was not adequate enough after a fixed number I of iterations, we made the algorithm restart, using another stochastic initial solution. Fig. 7 gives the numbers of iterations and trials needed to reach a solution such that, when substituted into the final nonlinear system, gives rise to a square norm of the residual less than 1%, for different values of the constant A, i.e., the number of harmonics considered in the series truncation (12). In this case, a nonlinear dielectric scatterer of dimensions $\lambda_0/30 \times \lambda_0/15 \times \lambda_0/30$ and characterized by $\varepsilon_b = 2.0$ and $\alpha_2 = 0.01$ was considered. Moreover, we assumed $I = 25$. For the scattering parallelepiped in Fig. 6(a), Fig. 8(a) gives the numbers of iterations and trials (needed to obtain the same accuracy as reported above) versus the values of the nonlinear index α_2. In this case, we assumed $A = 6$, $\varepsilon_b = 2.0$ and $I = 40$. Finally, Fig. 8(b) gives the numbers of iterations and trials for different values of the linear part of the relative dielectric permittivity, ε_b, for $A = 6, \alpha_2 = 0.1$ and $I = 40$.

IV. Conclusion

A numerical approach has been presented for the solution of the direct scattering problem in the case where electromagnetic waves are incident on a three-dimensional bounded dielectric object whose dielectric permittivity depends on the internal electric field. The approach is based on an integral-equation formalism that takes into account the nonlinear effect by means of equivalent sources. The moment method is used to discretize the resulting set of coupled integral equations.

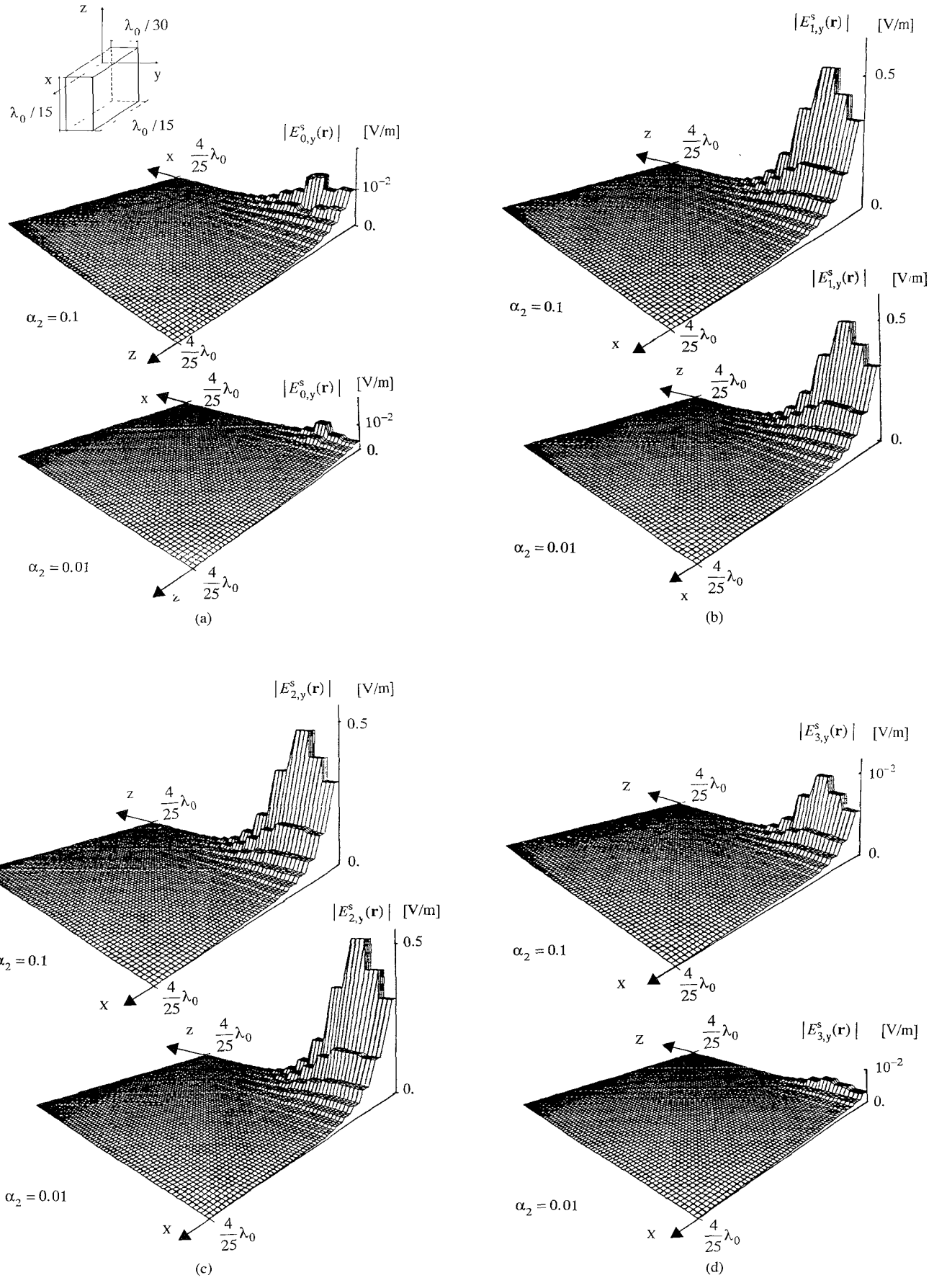

Fig. 6. Amplitudes of the harmonic components of theforward-scattered electric field ($\alpha_2 = 0.1$ and 0.01, $\varepsilon_b = 2.0, A = 6$): (a)0-th-order component (static field); (b) component at thefundamental frequency f_0; (c) $2f_0$; (d) $3f_0$. (e) $4f_0$ (1 testing point: 16 image pixels).

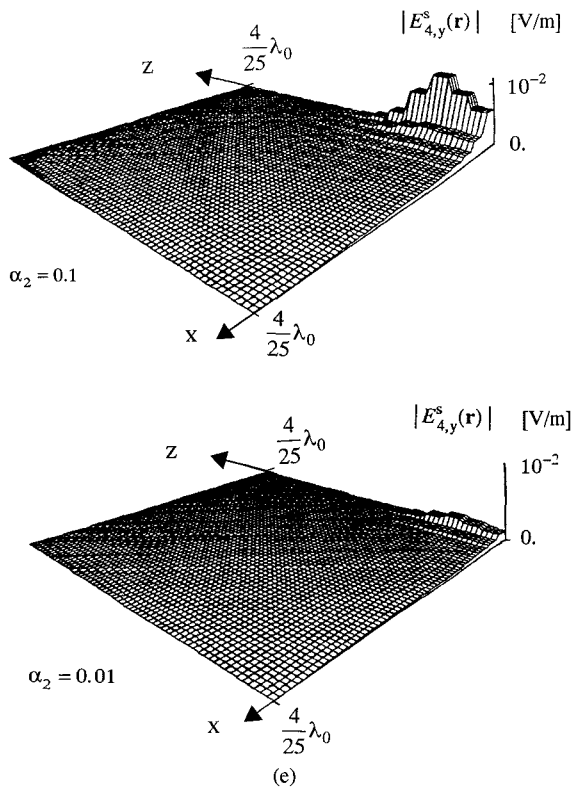

(e)

Fig. 6. *(Cont.)*

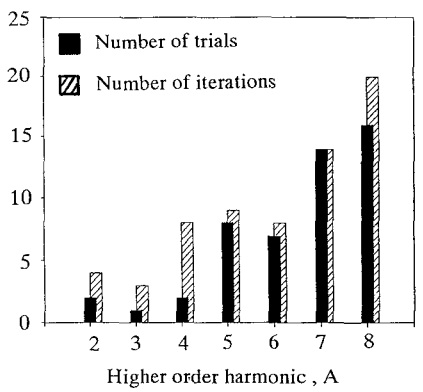

Fig. 7. Numbers of trials (black towers) and iterations (ruled towers) for different values of A (highest-order harmonic component) and for $\alpha_2 = 0.01$, $\varepsilon_b = 2.0, I = 25$.

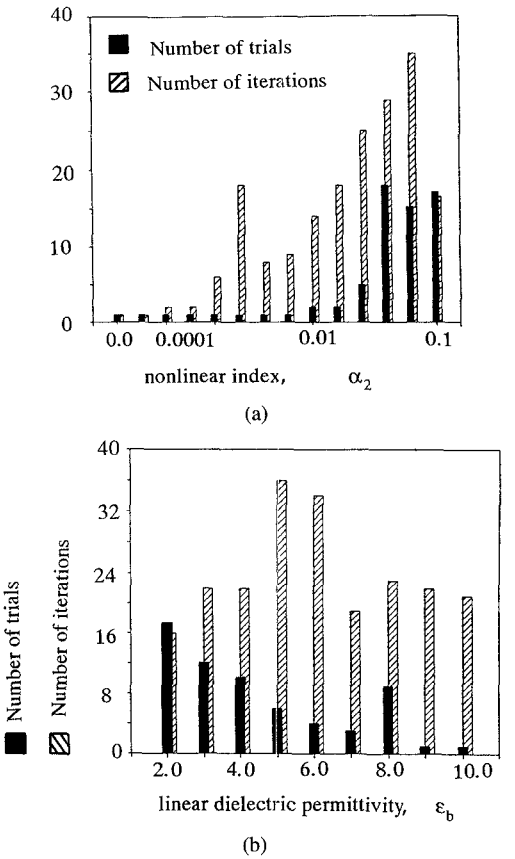

Fig. 8. Numbers of trials (black towers) and iterations (ruled towers): (a) versus the α_2 values, for$\varepsilon_b = 2.0, A = 6, I = 40$; (b) versus the ε_b values, for $\alpha_2 = 0.1, A = 6, I = 40$.

Wolfe's iterative method is applied to solve the final algebraic system of nonlinear equations.

The numerical results reported, although preliminary, seem to indicate the possibility of predicting the distributions of the harmonic components of the scattered electromagnetic fields inside and outside nonlinear scatterers of arbitrary shapes, for which analytical techniques cannot be used. Of course, due to the complexity of the electromagnetic problem considered, which is handled by the moment method, notable computation resources are required for the solution. The crucial point is the solution of the algebraic system of nonlinear equations. To this end, future work will be aimed at improving computation efficiency by applying other more appropriate solution algorithms. In particular, a computer code based on the simulated annealing method is currently under development. Moreover, it will be very important to obtain experimental data in order to verify the validity of the overall approach.

REFERENCES

[1] I. G. Katayev, *Electromagnetic Shock Wave.* London: Iliffe, 1966.
[2] A. Jeffrey and V. Korobeinikov, "Formation and decay of electromagnetic shock waves," *ZAMP*, vol. 20, pp. 440–447.
[3] A. Geffrey, "A brief history of solitons," in *Proc. 5th Int. Meeting 'Waves and Stability in Continuous Media,'* vol. 4, pp. 204–218, 1989.
[4] I. M. Besieris, "Solitons in randomly inhomogeneous media," in *Nonlinear Electromagnetics*, P. L. E. Uslenghi, Ed. New York: Academic, 1980, pp. 87–116.
[5] S. F. Liu and W. S. Wang, "Excitation of three-dimensional solitary waves from a nonlinear slab waveguide," *Microwave and Optical Technol. Lett.*, vol. 5, no. 10, pp. 517–520, Sept. 1992.
[6] S. F. Liu, P. K. Wei, and W. S. Wang, "A new approach to the analysis of the soliton: nonuniform finite difference beam propagation method," *Microwave and Optical Technol. Lett.*, vol. 5, no. 6, pp. 284–288, June 1992.
[7] N. D. Bloembergen, Ed., *Nonlinear Optics.* New York: Plenum, 1960.
[8] P. G. Harper and B. S Wherret, Eds., *Nonlinear Optics.* New York: Academic, 1977.
[9] P. L. E. Uslenghi, Ed., *Nonlinear Electromagnetics.* New York: Academic, 1980.
[10] A. Korpel and P. P. Banerjee, "A heuristic guide to nonlinear dispersive wave equations and soliton-type solutions," *Proc. IEEE*, vol. 72, pp. 1109–1130, 1984.
[11] Special issue of *J Optical Society of America B* on "Nonlinear Guided-Wave Phenomena," vol. 5, no. 2, Feb. 1988.
[12] J. B. Keller and M. H. Millman, "Perturbation theory of nonlinear electromagnetic wave propagation," *Phys. Rev.*, vol. 181, no. 5, pp. 1730–1747, May 1969.

[13] E. Bedrosian and S. O. Rice, "The output properties of Volterra systems (nonlinear systems with memory) driven by harmonic and Gaussian inputs," *Proc. IEEE*, vol. 59, pp. 1688–1707, 1971.
[14] D. C. Dalpe, G. Kent, and D. D. Weiner, "Extension of Volterra analysis to weakly nonlinear electromagnetic field problems with applications to whistler propagation," *IEEE Trans. Microwave Theory Tech.*, vol. MTT-30, pp. 1059–1067, July 1982.
[15] T. K. Sarkar and D. Weiner, "Scattering analysis of nonlinearly loaded antennas," *IEEE Trans. Antennas Propagat.*, vol. AP-24, no. 2, pp. 125–131, 1976.
[16] D. Censor, "Scattering by weakly nonlinear objects," *SIAM J. Appl. Math.*, vol. 43, pp. 1400–1417, 1983.
[17] ——, "Harmonic and transient scattering from weakly nonlinear objects," *Radio Sci.*, vol. 22, no. 2, pp. 227–233, Mar.–Apr. 1987.
[18] M. A. Hasan and P. L. E. Uslenghi, "Electromagnetic scattering from nonlinear anisotropic cylinders—Part I: Fundamental frequency," *IEEE Trans. Antennas Propagat.*, vol. 38, no. 4, pp. 523–533, Apr. 1990.
[19] ——, "Higher-order harmonics in electromagnetic scattering from a nonlinear anisotropic cylinder," *Electromagnetics*, vol. 11, pp. 377–392, 1991.
[20] R. F. Harrington, *Field Computation by Moment Method.* New York: McMillan, 1968.
[21] J. H. Richmond, "Scattering by a dielectric cylinder of arbitrary cross-section shape," *IEEE Trans. Antennas Propagat.*, vol. 13, pp. 334–341, 1965.
[22] C. T. Tai, *Dyadic Green's Functions in Electromagnetic Theory.* Scranton: Int. Textbooks, 1971.
[23] D. E. Livesay and K. M. Chen, "Electromagnetic fields inside arbitrarily shaped biological bodies," *IEEE Trans. Microwave Theory Tech.*, MTT-22, pp. 1273–1280, 1974.
[24] J. Van Bladel, "Some remarks on Green's dyadic for infinite space," *IRE Trans. Antennas Propagat.*, vol. AP-9, pp. 563–566, Nov. 1961.
[25] P. Wolfe, "The secant method for simultaneous nonlinear equations," *Commun. ACM*, vol. 2, no. 12, pp. 12–13, 1959.

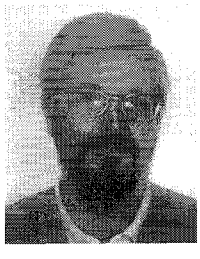

Salvatore Caorsi received the "laurea" degree in electronic engineering from the University of Genoa, Genoa, Italy, in 1973.

After graduation he remained at the University as a researcher, and since 1976 he has been professor of antennas and propagation. In 1985 he also assumed the title of professor of fundamentals of remote sensing. He is with the Department of Biophysical and Electronic Engineering, where he is responsible for the Applied Electromagnetics Group and for the Inter-University Research Center for Interactions Between Electromagnetic Fields and Biological Systems (ICEMB). His primary activities are focused on applications of electromagnetic fields to telecommunications, artificial vision and remote sensing, biology, and medicine. In particular, he is working on research projects concerning microwave hyperthermia and radiometry in oncological therapy; numerical methods for solving electromagnetic problems; and inverse scattering and microwave imaging.

He is a member of the Associazione Elettrotecnica ed Elettronica Italiana (AEI), of the European Bioelectromagnetism Association (EBEA), and of the European Society for Hyperthermic Oncology (ESHO).

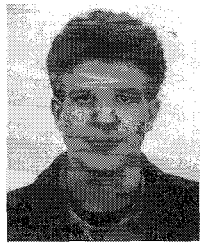

Andrea Massa is a Ph.D. student of electronics and computer science in the Department of Biophysical and Electronic Engineering, University of Genoa, Genoa, Italy. He received the "laurea" degree in electronic engineering from the University of Genoa in 1992. Since that year, he has cooperated in the activities of the Applied Electromagnetism Group.

His main interests are in the field of electromagnetic direct and inverse scattering, biomedical applications of electromagnetic fields, nonlinear wave propagation, and numerical methods in electromagnetism.

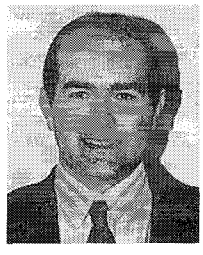

Matteo Pastorino (M'90) received the "laurea" degree in electronic engineering from the University of Genoa, Genoa, Italy, in 1987 and the Ph.D. degree in Electronics and Computer Science from the same university in 1992.

Since 1987, the year it was established, he has cooperated on the activities of the Inter-University Research Center for Interactions Between Electromagnetic Fields and Biological Systems and the Applied Electromagnetics Group. At present he is an assistant professor of Electromagnetic Fields in the Department of Biophysical and Electronic Engineering. His main research interests are in electromagnetic direct and inverse scattering, microwave imaging, wave propagation in presence of nonlinear media, and in numerical methods in electromagnetism. He is also working on research projects concerning biomedical applications of e.m. fields and microwave hyperthermia.

He is a member of the Associazione Elettrotecnica ed Elettronica Italiana (AEI), and of the European Bioelectromagnetism Association (EBEA).